2021 IEEE 15th International Symposium on Applied Computational Intelligence and Informatics (SACI) | 978-1-7281-9544-5/20/$31.00 ©2021 IEEE | DOI: 10.1109/SACI51354.2021.9465564

Human Computer Interaction Feedback Based-On Data Visualization Using MVAR and NN

J. I. Olszewska

University of West Scotland, UK

joanna.olszewska@ieee.org

***Abstract*—In the situation of pandemic with people being ill, contagious, or suffering from long-term effects, touchless human computer interfaces, and especially brain computer interfaces (BCI), could provide humans with safe communication technologies as well as user-centric systems for rehabilitation. Hence, this work studies at first the representation of electroencephalogram (EEG) signals in a data space which is appropriate for an efficient data processing and a user-friendly interpretation. Then, we propose 3D data visualizations mapping the human brain activity into that data space. The developed representations have been successfully tested within a BCI framework through 3D data visualizations the user can see and interact with in real time.**

***Index Terms*—Human Computer Interaction; Brain Computer Interface; Assistive Technology; Multi-Variate Signal Processing; Data Processing; Data Visualization; Machine Learning; Neural Networks; Reinforcement Learning; 3D Visual Feedback; User-Center Graphical Interface.**

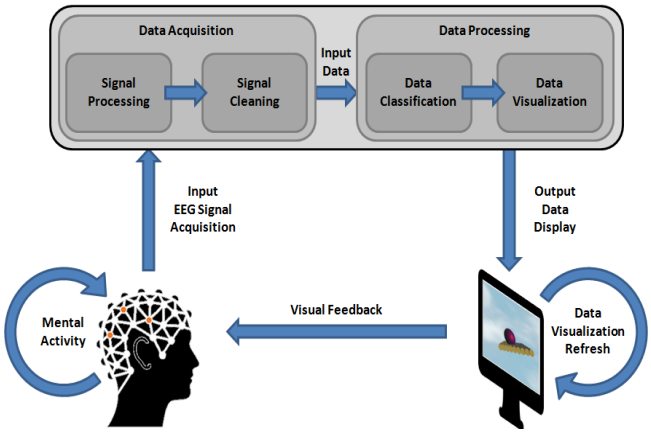

Fig. 1. Overview of the developed BCI system.

I. Introduction

Nowadays, developing safe human computer interfaces (HCIs) is of prime importance [1]. In particular, brain computer interfaces (BCIs) [2] can offer touch-free communication and/or control systems [3] and play a cornerstone role in assistive technologies [4] as well as rehabilitation systems [5], providing thus human-centric IT solutions for challenges like Covid-19 related-situations [6].

Indeed, BCI is defined as a HCI that does not depend on the brain's normal output pathways of peripheral nerves and muscles [7], but that directly relies on bio-electrical signals, which are generated by mental activities, to action IT features on computers [8], machines [9], smartphones [10], or robots [11], leading to a mind-based communication system [12].

Actually, BCI is not a mind-reading process, but a signal-processing system which allows touch-free control that can be used in multimedia communication applications [13], such as web browsers [14], video players [15], musical interface controllers [16], virtual reality (VR) games [17], biometric recognition tools [18], in learning [19] and neurorehabilitation techniques [20], or in assistive technologies [21], such as spellers [22], wheelchairs [23], or even smart homes [24].

Most of these BCIs have been designed as signal processing systems [25], which acquire user's electroencephalogram (EEG) signals and process them at first by removing noise in a pre-processing phase, e.g. by applying Principal Component Analysis (PCA) on the acquired EEG signals [26], then by performing a feature extraction, e.g. using Fast Fourier Transform (FFT) [27] to derive feature vectors. Next, these latter ones are identified as corresponding to a cognitive task generating an output command or not, by means of classifiers involving, e.g. Linear Discriminant Analysis (LDA) [28] or Support Vector Machines (SVM) [29].

With all the ongoing development of machine learning (ML) in the healthcare domain [30] and related assistive technologies [31], recent BCI studies [32] started to look at ML for BCI. Hence, in this work, we consider BCI as a data processing system, with two main units, one for data acquisition and one for data processing, as depicted in Fig. 1. Furthermore, our BCI data processing system is a closed-loop process where the data inputs are generated by the user through cognitive tasks, and the data outputs are visualized on a computer display, providing the user with a real-time visual feedback.

Such BCI data processing system requires thus adapted data visualization which could be of different type and nature, in order to provide a meaningful and user-friendly feedback to the user, e.g. in the training phase and during application.

The most common BCIs have provided users with visual feedback that could be discrete or continuous [33]; symbolic, e.g. presenting one-dimensional (1D) indicator [34] or displaying two-dimensional (2D) scenes [35]; realistic, e.g. involving augmented reality (AR) [36]; or virtual, e.g. calling upon virtual reality (VR) [2].

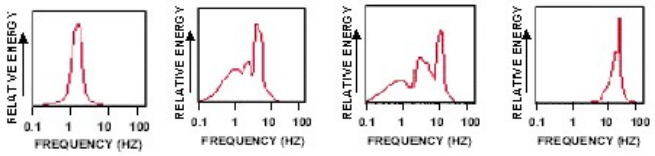

(a) (b) (c) (d)

Fig. 2. Brainwaves of band (a) delta; (b) theta; (c) alpha; (d) beta.

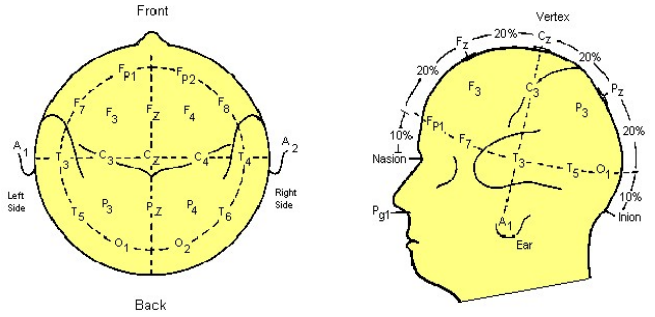

Fig. 3. View of the *10-20 international system* of electrode arrangement over the human scalp.

While the importance of visual feedback in the BCI process has been established [37], little has been studied about the design and development of abstract three-dimensional (3D) data visualizations to sustain the BCI data process.

Hence, in this paper, we present new data visualizations for BCI systems, where the visualization of the features of the cerebral electrical activity aims to facilitate the interpretation of EEG data and to close the loop in the BCI system, while fostering real-time interaction.

Our visualizations provide 3D visual feedbacks, which are integrated within a BCI data processing prototype, in order to study their real-world performance.

It is worth noting that BCIs can capture human bio-electrical activity in different ways, leading to invasive BCI [38], hybrid BCI [39], wireless BCI (WBCI) [40], or non-invasive BCI systems [41]. The latter ones do not require user's surgery or permanent attachment to the measuring device. Hence, in this work, our BCI system measures the user's brain activity non-invasively through electroencephalogram (EEG) signal.

EEG signal corresponds to the spontaneous electrical activity of the cerebral cortex and has a high temporal resolution capable of measuring every thousandth of a second. Furthermore, EEG signal can be decomposed in four frequency bands, leading to brainwaves (Fig. 2), namely, delta waves [1-4Hz], theta waves [5-7Hz], alpha waves [8-13Hz], and beta waves [14-20Hz] [27]. Delta waves have an amplitude which is included between 20 and 200 μVolt. These brainwaves are present during the deep sleep, also called slow-wave sleep. Theta waves have an amplitude of 5 to 100 μVolt and appear during drowsiness and early slow-wave sleep or light sleep. Alpha waves of moderate amplitude, i.e. within the range of 5-100 μVolt, are typical of relaxed wakefulness (idling) as well as creativity. Lower-amplitude beta waves are more prominent during intense mental activity involving concentration or stress.

On the other hand, EEG has a reasonable spatial resolution, as signals from up to 256 electrode sites can be measured at the same time. In particular, we adopt the 10-20 international standard for electrode placement on the human scalp, as defined by the International Federation in Electroencephalography and Clinical Neurophysiology. In the 10-20 international system (Fig. 3), even numbers indicate electrodes located on the right side of the head, and odd numbers indicate those on the left side; the index z being dedicated to an electrode located on the line separating the two sides. Capital letters are used to reference each cortical zone, namely, frontal (F), central (C), parietal (P), temporal (T), and occipital (O). (Fp) and (A) stand for frontal pole and auricular, respectively [41].

Besides, BCIs require the adoption of a *mental strategy*, i.e. cognitive tasks to generate EEG components through voluntary and conscious mental activity. Such mental strategy could involve *motor imagery* (MI) (e.g. imagining left or right hand movement) [34] or another *mental activity* (MA) (e.g. performing arithmetic operations) [29]. In this work, we opt for the latter ones. Indeed, the MAs used for our BCI have been chosen in accordance with brain hemispheric studies [29] which suggest that the two hemispheres of the human brain are specialized for different cognitive functions; the left hemisphere being predominantly involved in verbal and other analytical functions, while the right one in spatial and holistic processing.

In our BCI system, the different data visualizations associated with these MAs follow a user-centric design, involving continuous and timely visual feedback which focuses on a closed foreground and presents a simple background.

Moreover, our data visualizations allow user-friendly, MA-based BCI systems for touchless communication and control of IT smart tools.

Thence, the contribution of this paper is twofold. On one hand, we consider BCI in terms of data processing and, on the other hand, we elaborate three data visualizations of human EEG signals in real time, in order to provide user-friendly and user-centric 3D visual feedback for people in context of assistive and rehabilitation technologies.

The paper is structured as follows. In Section II, we present our brain-computer data acquisition, processing, and visualization, while in Section III, we use this BCI data system for cognitive training and mental activity recognition and we report the related experimental results. Conclusions are drawn up in Section IV.

II. Developed BCI System

In this section, we describe our MA-based BCI as a data processing system (Fig. 1). The proposed touch-free BCI data system has two main units, namely, data acquisition unit and data processing unit, as explained in Sections II-A and II-B, respectively. The data acquisition unit encompasses signal acquisition, processing, and cleaning, while the data processing unit covers data classification and visualization.

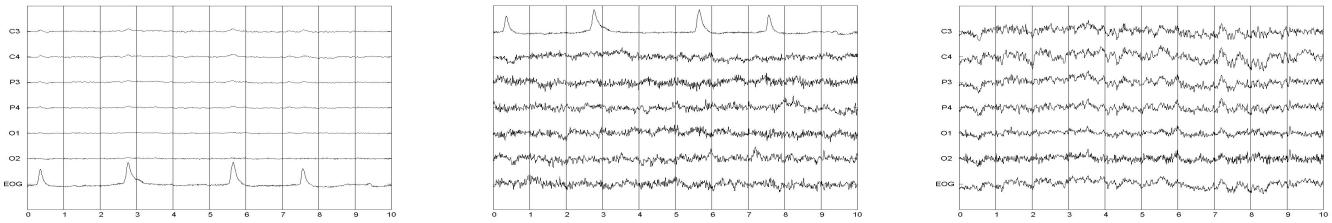

(a) (b) (c)

Fig. 4. Sample of EEG signals which are (a) first acquired, (b) then decomposed using ICA, and (c) next cleaned to remove noise such as eye blinking. These EEG signals have been recorded at the C3, C4, P3, P4, O1, and O2 electrodes that correspond to the central zone of the cerebral activity.

A. Data Acquisition

The data acquisition unit consists of three phases that comprise signal acquisition, processing, and cleaning (Fig. 4).

Hence, the user starts to perform MAs, and the corresponding EEG signals are acquired by an electrode array, which is arranged according to the 10-20 international system, and a digitization device. In regards to their biomedical properties, the acquired EEG signals are a multidimensional stochastic process with non-zero mean.

In EEG data acquisition, a mental activity (MA) is represented as a matrix X, where each row corresponds to the EEGs which are recorded at a particular electrode, while the columns represent the measures at the different instants. In Fig. 4(a), the total duration of the acquired EEG signals is of 10s, and the sampling frequency is of 250Hz.

These acquired EEG signals are a mixture of the basic components of the cerebral activity, similar to the 'cocktail-party effect'. Thus, the aim of the signal processing phase is to decompose the acquired EEG signal, i.e. to recover the original components of the cerebral activity from the acquired mixed signal.

For that, we apply the independent component analysis (ICA) [42] to linearly decompose the multivariate signal S into independent source components, as shown in Fig. 4(b). Thence, ICA produces the matrix W, where the columns of W^{-1} represent the intensity of the projections which are related to each electrode, as follows:

$$S = W^{-1} \cdot X. \tag{1}$$

Since EEG signals can be corrupted by noise due to eye blinking, eye movements, or muscular artifacts [43], EEG signals should be 'cleaned', as in Fig. 4(c). Hence, we use ICA to remove this potential noise, leading to:

$$\widetilde{X} = \widetilde{W} \cdot S. \tag{2}$$

B. Data Processing

The data processing consists in data classification and data visualization; the choice of the features to characterize the cerebral activity depending of the data visualization. This implies that the number of these features cannot be high in order to ensure a user-friendly data visualization and consequently, an easy interpretation for the human in the loop. For this purpose, we developed three different approaches for data representation (Fig. 5), as follows.

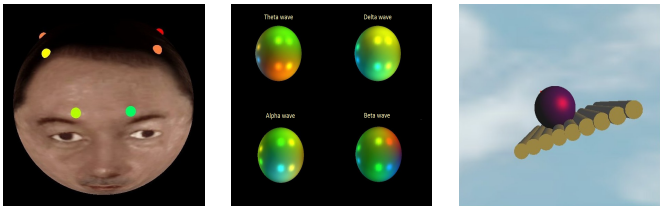

(a) (b) (c)

Fig. 5. BCI data visualizations called (a) *ViewAll*, (b) *Head*, and (c) *Sisyphus*, respectively. Better viewed in colour.

1) ViewAll Approach: The idea underpinning this 3D data visualization (Fig. 5(a)) is to enable users to see their bio-electrical activity at each electrode in terms of 3D colour spotlights, which hue H is varying in real time with the total signal power P at the corresponding electrode; the adopted colour model being Hue(H)-Saturation(S)-Brightness(B) (HSB).

Indeed, the cerebral activity can be characterized by the power of EEG signals at each electrode. The total power P is computed over all the channels with a sampling frequency of 250Hz and n = 0.5s, as follows:

$$P = \frac{1}{n} \sum_{i=1}^{125} |X_i|^2. \tag{3}$$

In the *ViewAll* approach, we search for a linear relation between H and P. The observation of the HSB colour wheel (Fig. 6), given S and B, leads to the following conditions: (i) the red hue corresponds to the maximum power, while the blue hue indicates the minimum power; (ii) the colour hue is moving clockwise on the HSB colour wheel, i.e. from blue to red, through green and yellow, and avoiding magenta hue.

The normalization of the power simplifies the relation without loss of generality. The relation becomes then:

$$y = \frac{0° - 225°}{360°} \cdot x + \frac{225°}{360°} = -0.625 \cdot x + 0.625. \tag{4}$$

Hence, in the *ViewAll* visualization, each electrode is symbolized by a spotlight as per Eq. 4, while the location of

Fig. 6. Hue Saturation Brightness (HSB) colour model wheel.

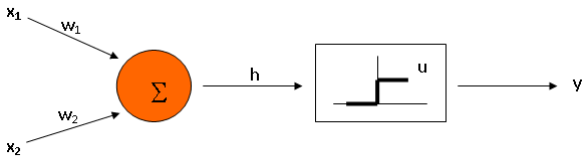

Fig. 7. Artificial neural network (ANN).

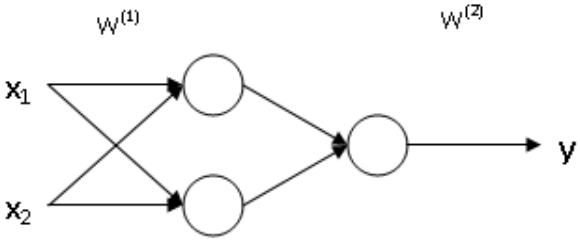

Fig. 8. Two-layer perceptron.

the electrode is computed, as follows. At first, the Cartesian electrode coordinates, as provided in the 10-20 international system, are normalized: $(x, y, z) \rightarrow (\hat{x}, \hat{y}, \hat{z})$, with $R = \sqrt{x^2 + y^2 + z^2}$. Next, in order to get the appropriate orientation, they are transformed, as follows:

$$\begin{cases} x & = -\hat{y} \\ y & = \hat{z} \\ z & = -\hat{x}. \end{cases} \tag{5}$$

ViewAll visualization consists thus in the linear association of the input total power P and the hue H of spotlights that symbolize the electrodes and that light a head model which point of view can be changed to further visualize the data.

2) Head Approach: The idea behind this 3D data visualization (Fig. 5(b)) is similar to the previous one, but here, we look at the power in the four frequency bands of the characteristic brainwaves, namely, delta, theta, alpha and beta waves, rather than at the total power. EEG signal processing consists then in applying FFT [27] to the signals and to compute the power in the respective four frequency bands, similarly to Eq. 3.

This *Head* visualization allows thus to simultaneously see the power of each of the delta, theta, alpha and beta brainwaves on the respective floodlit sphere which symbolizes a human head. Each spotlight represents a particular electrode. Its hue is a linear function of the corresponding brainwave power, as per Eq. 4. Moreover, the spotlights are far away from each sphere, and they light locations corresponding to FP2, C4, P4 as well as FP1, C3, P3 electrodes, which are above and below the sphere, respectively. For this visualization, the electrode coordinates are provided by:

$$\begin{cases} x & = far \cdot \hat{x} \\ y & = far \cdot \hat{y} \\ z & = far \cdot \hat{z}, \end{cases} \tag{6}$$

with far, the distance between a spotlight and the sphere.

3) Sisyphus Approach: The principle governing this 3D data visualization (Fig. 5(c)) is as follows. At the beginning, a ball is resting at the bottom of a sloping surface. When the user performs an MA, the ball moves up the slope. In case the user is idling, stopping, or changing of MA, the ball starts to go down the slope.

The *Sisyphus* representation considers the EEG signals as a multi-dimensional stochastic process and relies on the multivariate auto-regressive (MVAR) model. The MVAR model of order p [44] can be formalized as follows:

$$v_k = w + \sum_{l=1}^{p} A_l v_{k-l} + \epsilon_k, \tag{7}$$

with $v_k \in \mathbf{R}^m$, state vectors observed at equally spaced k instants; $\epsilon_k = noise(C)$, uncorrelated random vectors with mean zero and covariance matrix $C \in \mathbf{R}^{m \times m}$, with m, the number of channels; $w \in \mathbf{R}^m$, vector allowing a non-zero mean of the observed vectors: $\langle v_k \rangle = (I - A_1 - ... - A_p)^{-1} w$; $A_l \in \mathbf{R}^{m \times m}$, the matrix of the MVAR model coefficients that are useful for the visualization.

It is worth noting that the function `arfit` of the MatLab ARFIT toolbox [45] searches for the optimum order p getting the least error in terms of least squares, given a minimum model order p_{min} and a maximum model order p_{max}.

In our work, k=0.5s, f_e=250Hz, T=125, m=2, and p=2.

As the matrix A is composed of p matrices of size $m \times m$, each MA is, in our case, entirely characterized in a eight-dimensional space. Since such space cannot be visualized, this latter one is projected on different planes which are determined by the coefficients selected two by two, in order to find a data space appropriate for visual interpretation. The data classification is then done by means of a non-linear classifier involving an artificial neural network (ANN) (Fig. 7). It allows to find the best couple of MVAR coefficients, leading to the highest MA recognition rate, i.e. to the highest selectivity or discrimination among the MAs.

The artificial neuron (AN) [46] computes a weighted sum of its n input signals x_j, with $j = 1, 2, ..., n$, as follows:

$$y = \theta \left(\sum_{j=1}^{n} w_j x_j - u \right), \tag{8}$$

where $\theta()$ is an activation function such as the step function, and w_j is the synapse weight associated with the jth input.

Algorithm 1 Back-Propagation Algorithm

1. Initialize the weights to small random values.
2. Randomly choose an input value x^{μ}.
3. Propagate the signal forward through the network.
4. Compute $\delta_i^L = g'\left(h_i^L\right)\left[d_i^u - y_i^L\right]$ in the output layer $\left(o_i = y_i^L\right)$, where h_i^l represents the net input to the ith unit in the lth layer, and g' is the derivative of the activation function g.
5. Compute the deltas for the preceding layers by propagating the errors backwards: $\delta_i^l = g'\left(h_i^l\right)\sum_j w_{ij}^{l+1}\delta_j^{l+1}$ for $l = (L-1), ..., 1$.
6. Update weights using $\Delta w_{ji}^l = \eta\delta_i^l y_j^{l-1}$.
7. Repeat steps 2-6 for the next value until the error in the output layer is below a specified threshold or a maximum number of iterations is reached.

The AN output is 1, if this sum is above a threshold u, and otherwise, the output is 0. Hence, in our case, if the input x belongs to the idling class, the result is equal to 1, and if the input x represents another MA, the output is 0; the input x corresponding to one of the 28 combinations of the MVAR coefficients picked two by two. We adopt thus a multi-layer perceptron (MLP) model, since MLPs have been proven to be more efficient than convolutional neural networks (CNNs) [2], and in our MLP, the number of layers is two, leading to a two-layer perceptron (Fig. 8). For the layer 1, we choose a sigmoid function as activation function defined by $g(x) = 1/(1 + exp(-\omega x))$, where ω is the slope parameter. For the layer 2, we keep the step function at 0. For the ANN learning algorithm, we choose the back-propagation algorithm, which adjusts the weights based on error-correction rules. This NN training algorithm is detailed in Algorithm 1.

After this data classification, the data based on user's MAs can be visualized using the proposed *Sisyphus* visualization, which viewpoint can be changed to ensure a greater freedom in the data visualization.

It is worth noting that data classification has been coded in MatLab and used NN [47] as well as ARFIT libraries [45], while data visualization has been produced using Java programming language and Java 3D library [48]. Java 3D is a scene graph-based 3D application programming interface (API) for the Java platform, running on top of either OpenGL or DirectX and enabling the portability of the data visualization. Hence, each data visualization was encoded as a Java 3D scene graph which was represented by a directed acyclic graph (DAG). Figure 9 presents the DAGs that correspond to the three developed data visualizations.

III. Results and Discussion

In order to validate our developed user-centric 3D data visualizations for the BCI data system, experiments have been carried out with two subjects who participated in five sessions of twenty minutes. Each 20-minute session was split in two 10-minute experiments, using at first, *ViewAll* and *Head* data visualizations and then, *Sisyphus* data visualization; all described in Section II. During these experiments, each user was wearing an EEG cap with six electrodes which were placed according to the 10-20 international system and connected to the BCI system set-up as depicted in Fig. 1.

TABLE I
Recognition rate results that are obtained with different classifiers in case of different mental activities (MA).

Classifier Type	Idling Recognition	MA Recognition
Linear Classifier	96%	50%
Non-Linear Classifier	84%	82%

In each session, the user was asked to perform three MAs such as 'relaxation' (i.e. 'idling'), 'multiplication', or 'count', while getting real-time visual feedback about his/her cognitive activities via the respective, developed 3D data visualization.

As reported in Table 1, idling is recognized at 96%, and the recognition rate between idling and the other MAs is 50%, when using a linear classifier as for *ViewAll* and *Head* data visualizations. On the other hand, idling is recognized at 84%, and the highest selectivity or discrimination among the MAs is 82%, in the case of the MLP non-linear classifier as for *Sisyphus* data visualization. We can also observe that the two-layer perceptron achieves the best results in classifying the cognitive tasks, i.e. the highest MA recognition rate, with the (A_{22}, A_{24}) MVAR coefficient couple, while idling is better recognized using the (A_{13}, A_{22}) MVAR coefficient couple.

From the HCI designer' point of view, the study demonstrates there is an interdependency between the data features/ classifiers and the data visualization, while from the user's point of view, it appears from the experiments that the BCI performance in the recognition of the different MAs is influenced by the data visualization which provides the real-time visual feedback and acts as a computer-animated virtual environment.

Therefore, *ViewAll* and *Head* data visualizations, which call on the feature of the acquired EEG signals' total power and power in each of the four frequency bands, respectively, present a linear relation between the input data power at an electrode and the output data hue of a spotlight on a sphere, allowing users' observation of their own bio-electrical cerebral activity in real time. These 3D data visualizations are thus recommended for calibration and familiarization of the user with the BCI system.

The *Sisyphus* data visualization stages a ball going up or down, depending if the user is resting or performing MAs such as arithmetic operations. The user can thus interact with the BCI system by moving the ball in one direction or another by means of his/her state of mind. This visualization, which involves the MVAR model, uses a non-linear NN classifier to efficiently recognize the user's relaxation state from other MAs, leading to real-time users' observation of their own mental activity; such visualization being useful in situations of user's learning and training of the BCI system.

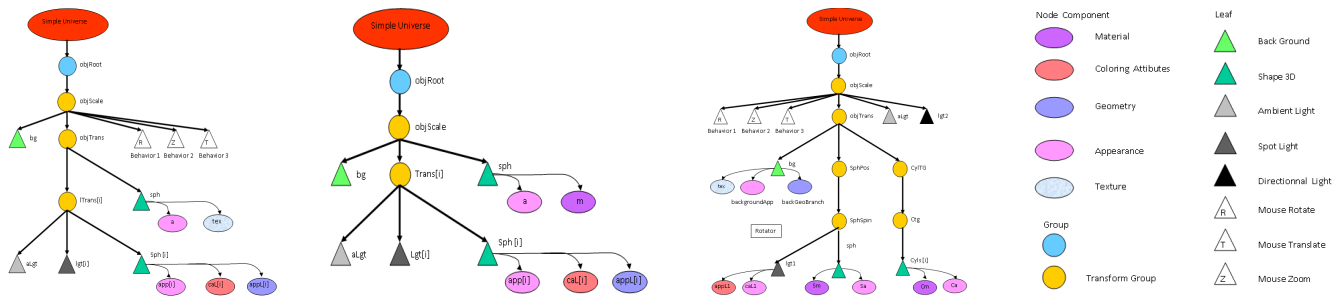

(a) (b) (c) (d)

Fig. 9. Java 3D scene graph as a directed acyclic graph (DAG) for (a) *ViewAll*, (b) *Head*, and (c) *Sisyphus* data visualization, respectively; (d) the legend (better viewed in colour).

IV. Conclusions

Brain Computer Interfaces (BCI) started to be studied in order to visualize mind activity, while their recent application is to communicate and control smart technologies in a touch-less way. This type of HCI is thus of high benefit in case of pandemics such as Covid-19 and/or assistive/rehabilitation processes, e.g. from Long Covid. For this purpose, we have presented, in this paper, a non-invasive and user-centric BCI data processing system, where data are acquired from EEG signals that are generated by user's mental activity (MA). In the data acquisition unit, this input data is decomposed and cleaned by techniques such as ICA, before being transferred as MVAR signals of order 2 to the data processing unit where machine learning techniques involving NN are applied to this data in order to recognize MAs such as relaxation, multiplication, and count. This processed data is then visualized in real time thanks to our user-friendly 3D data visualizations which provide the user with a visual feedback, closing thus the loop in the BCI system, and allowing the user to interact in real time with the system, leading to touch-free triggering of actions/commands in real-world systems.

Acknowledgments

Thanks go to Dr Gary Garcia for collecting the EEG data.

References

[1] S. Wilding, P. Walker, S. Clinton, D. Williams, and J. I. Olszewska, "Safe human-computer interface based on an efficient image processing algorithm", in *Proceedings of the IEEE International Symposium on Computational Intelligence and Informatics (CINTI)*, 2020, pp. 1-6.

[2] V. Rouanne, M. Sliwowski, T. Costecalde, A. L. Benabid, and T. Aksenova, "Detection of error correlates in the motor cortex in a long term clinical trial of ECoG based brain computer interface", in *Proceedings of the International Conference on Bio-Inspired Systems and Signal Processing (BIOSIGNALS)*, 2021, pp. 26-34.

[3] J. R. Wolpaw, N. Birbaumer, D. J. McFarland, G. Pfurtscheller, and T. M. Vaughan, "Brain-computer interfaces for communication and control", *Clinical Neurophysiology*, vol. 113, no. 6, pp. 767-791, 2002.

[4] V. Gandhi, *Brain-Computer Interfacing for Assistive Robotics*, Academic Press, 2014.

[5] E. Maiorana, J. Sole-Casals, and P. Campisi, "EEG signal preprocessing for biometric recognition", *Machine Vision and Applications*, vol. 27, no. 8, pp. 351-360, 2016.

[6] M. Sharma, "Design of brain-computer interface-based classification model for mining mental state of COVID-19 afflicted mariner's", *International Maritime Health*, vol. 71, no. 4, pp. 298-300, 2020.

[7] J. R. Wolpaw, N. Birbaumer, W. J. Heetderks, D. J. McFarland, P. H. Peckham, G. Schalk, E. Donchin, L. A. Quatrano, C. J. Robinson, and T. M. Vaughan, "Brain-computer interface technology: A review of the first international meeting", *IEEE Transactions on Rehabilitation Engineering*, vol. 8, no. 2, pp. 164-173, 2000.

[8] K. C. Tseng, Y.-T. Wang, B.-S. Lin, and P. H. Hsieh, "Brain computer interface-based multimedia controller", in *Proceedings of the IEEE International Conference on Intelligent Information Hiding and Multimedia Signal Processing*, 2012, pp. 277-280.

[9] W. He, Y. Zhao, H. Tang, C. Sun, and W. Fu, "A wireless BCI and BMI system for wearable robots", *IEEE Transactions on Systems, Man, and Cybernetics: Systems*, vol. 46, no. 7, pp. 936-946, 2016.

[10] S. R. A. Jafri, T. Hamid, R. Mahmood, M. A. Alam, T. Rafi, M. Z. U. Haque, and M. W. Munir, 'Wireless brain computer interface for smart home and medical system", *Wireless Personal Communications*, vol. 106, pp. 2163-2177, 2019.

[11] A. Nourmohammadi, M. Jafari, and T. O. Zander, "A survey on unmanned aerial vehicle remote control using brain-computer interface", *IEEE Transactions on Human-Machine Systems*, vol. 48, no. 4, pp. 337-348, 2018.

[12] F. Jabeen, L. Tao, and X. Wang, "Mind interactive multimedia system for disabled people", in *Proceedings of the IEEE International Conference on Congress on Image and Signal Processing, BioMedical Engineering and Informatics*, 2017, pp. 1-6.

[13] S. Bosse, K.-R. Muller, T. Wiegand, and W. Samek, "Brain-computer interfacing for multimedia quality assessment", in *Proceedings of the IEEE International Conference on Systems, Man, and Cybernetics (SMC)*, 2016, pp. 2834-2839.

[14] M. M. Moore, "Real-world applications for brain-computer interface technology", *IEEE Transactions on Neural Systems and Rehabilitation Engineering*, vol. 11, no. 2, pp. 162-165, 2003.

[15] E. Teo, A. Huang, Y. Lian, C. Guan, Y. Li, and H. Zhang, "Media communication center using brain computer interface", in *Proceedings of the IEEE International Conference of the IEEE Engineering in Medicine and Biology Society (EMBS)*, 2006, pp. 2954-2957.

[16] B. Arslan, A. Brouse, J. Castet, J.-J. Filatriau, R. Lehembre, Q. Noirhomme, and C. Simon, "Biologically-driven musical instrument", in *Proceedings of the Summer Workshop on Multimodal Interfaces (eINTERFACE)*, 2005, pp. 1-14.

[17] H.-L. Fu, P.-H. Fang, C.-Y. Chi, C.-T. Kuo, M.-H. Liu, H. M. Hsu, C.-H. Hsieh, S.-F. Liang, S. Hsieh, and C.-T. Yang, "Application of brain-computer interface and virtual reality in advancing cultural experience", in *Proceedings of the IEEE International Conference on Visual Communications and Image Processing (VCIP)*, 2020, pp. 351-354.

[18] M. Al-Sagban, O. El-Halawani, T. Lulu, H. Al-Nashash, and Y. Al-Assaf, "Brain computer interface as a forensic tool", in *Proceedings of the IEEE International Symposium on Mechatronics and its Applications*, 2008, pp. 1-5.

[19] A. T. Poulsen, S. Kamronn, J. Dmochowski, L. C. Parra, and L. K. Hansen, "EEG in the classroom: Synchronised neural recordings during video presentation", *Nature Scientific Reports*, vol. 7, pp. 1-7, 2017.

[20] K. K. Ang and C. Guan, "Brain-computer interfaces for neurorehabilitation of upper limb after stroke", *Proceedings of the IEEE*, vol. 103, no. 6, pp. 944-953, 2015.

[21] T. C. Major and J. M. Conrad, "A survey of brain computer interfaces and their applications", *Proceedings of the IEEE SOUTHEASTCON*, 2014, pp. 1-8.

[22] A. Rezeika, M. Benda, P. Stawicki, F. Gembler, A. Saboor, and I. Volosyak, "Brain-computer interface spellers: A review", *Brain Sciences*, vol. 8, no. 4, pp. 1-38, 2018.

[23] L. Bi, X.-A. Fan, and Y. Liu, "EEG-based brain-controlled mobile robots: A survey", *IEEE Transactions on Human-Machine Systems*, vol. 43, no. 2, pp. 161-176, 2013.

[24] H.-S. Cho, J. Goo, D. Suh, K. S. Park, and M. Hahn, "The virtual reality brain-computer interface system for ubiquitous home control", in *Proceedings of the Australian Joint Conference on Artificial Intelligence, LNAI 4304*, 2006, pp. 992-996.

[25] S. G. Mason and G. E. Birch, "A general framework for brain-computer interface design", *IEEE Transactions on Neural Systems and Rehabilitation Engineering*, vol. 11, no. 1, pp. 70-85, 2003.

[26] Y. Wang, P. Berg, and M. Scherg, "Common spatial subspace decomposition applied to analysis of brain responses under multiple task conditions: A simulation study", *Clinical Neurophysiology*, vol. 110, pp. 604-614, 1999.

[27] M. Ramzan and S. Dawn, "A survey of brainwaves using electroencephalography (EEG) to develop robust brain-computer interfaces (BCIs): Processing techniques and algorithms", in *Proceedings of the IEEE International Conference on Cloud Computing, Data Science and Engineering*, 2019, pp. 642-647.

[28] J. Sole-Casals, C. F. Caiafa, Q. Zhao, and A. Cichocki, "Brain-computer interface with corrupted EEG data: A tensor completion approach", *Cognitive Computation*, vol. 10, no. 6, pp. 1062-1074, 2018.

[29] G. Garcia, "BCI adaptation using incremental-SVM learning", in *Proceedings of the IEEE EMBS Conference on Neural Engineering*, 2007, pp. 337-341.

[30] P. Piros, T. Ferenci, R. Fleiner, P. Andreka, H. Fujita, L. Fozo, L. Kovacs, and A. Janosi, "Comparing machine learning and regression models for mortality prediction based on the Hungarian myocardial infarction registry", *Knowledge-Based Systems*, vol. 179, pp. 1-7, 2019.

[31] M. Quinn and J. I. Olszewska, "British sign language recognition in the wild based on multi-class SVM", in *Proceedings of the IEEE Federated Conference on Computer Science and Information Systems*, 2019, pp. 81-86.

[32] X. Gu, Z. Cao, A. Jolfaei, P. Xu, D. Wu, T.-P. Jung, and C.-T. Lin, "EEG-based brain-computer interfaces (BCIs): A survey of recent studies on signal sensing technologies and computational intelligence approaches and their applications", *IEEE/ACM Transactions on Computational Biology and Bioinformatics*, pp. 1-22, 2021.

[33] G. Pfurtscheller, "Brain-computer interface - state of the art and future prospects", in *Proceedings of the European Signal Processing Conference (EUSPICO)*, 2004, pp. 509-510.

[34] G. Pfurtscheller, C. Neuper, D. Flotzinger, and M. Pregenzer, "EEG-based discrimination between imagination of right and left hand movement", *Electroencephalography and Clinical Neurophysiology*, vol. 103, no. 6, pp. 642-651, 1997.

[35] V. R. Mercado-Garcia and L. M. Alonso-Valerdi, "The identity of the protagonist in brain-computer interfaces: A user-centered design approach", in *Proceedings of the IEEE International Conference on Electronics, Communications and Computers*, 2018, pp. 44-49.

[36] G. Li, Y. Lian, and G. Wang, "Live demonstration: Evaluation of consumer's preference using augmented reality and EEG", in *Proceedings of the IEEE Biomedical Circuits and Systems Conference*, 2016, pp. 133.

[37] G. Pfurtscheller, C. Neuper, and N. Birbaume, *Motor Cortex in Virtual Movements*, chapter "Human Brain-Computer Interface", pp. 367-401, CRC Press, 2005.

[38] M. J. Vansteensel, E. G. M. Pels, M. G. Bleichner, M. P. Branco, T. Denison, Z. V. Freudenburg, P. Gosselaar, S. Leinders, T. H. Ottens, M. A. Van Den Boom, P. C. Van Rijen, E. I. Aarnoutse, and N. F. Ramsey, "Fully implanted brain-computer interface in a locked-in patient with ALS", *New England Journal of Medicine*, vol. 375, no. 21, pp. 2060-2066, 2016.

[39] S. Amiri, R. Fazel-Rezai, and V. Asadpour, "A review of hybrid brain-computer interface systems", *Advances in Human-Computer Interaction*, pp. 1-8, 2013.

[40] S. Lee, Y. Shin, S. Woo, K. Kim, and H.-N. Lee, *Brain-Computer Interface Systems - Recent Progress and Future Prospects*, chapter "Review of Wireless Brain-Computer Interface Systems", pp. 215-238, InTech Open, 2013.

[41] P. Lahane, J. Jagtap, A. Inamdar, N. Karne, and R. Dev, "A review of recent trends in EEG based brain-computer interface", in *Proceedings of the IEEE International Conference on Computational Intelligence in Data Science*, 2019, pp. 1-6.

[42] A. Hyvarinen and E. Oja, "Independent Component Analysis: Algorithms and applications", *Neural Networks*, vol. 13, no. 4-5, pp. 411-430, 2000.

[43] E. Gallego-Jutgla, J. Sole-Casals, T. M. Rutkowski, A. Cichocki, "Application of multivariate empirical mode decomposition for cleaning eye blinks artifacts from EEG signals", in *Proceedings of the International Joint Conference on Computational Intelligence*, 2011, pp. 455-460.

[44] A. Neumaier and T. Schneider, "Estimation of parameters and eigenmodes of multivariates autoregressive models", *IEEE Transactions on Mathematical Software*, vol. 27, no. 1, pp. 27-65, 2001.

[45] J. F. Hair Jr, R. E. Anderson, R. L. Tatham, and W. C. Black, *Multivariate Data Analysis: A Global Perspective*, 7th Ed., Prentice Hall, 2009.

[46] A. K. Jain, J. Mao, and K. M. Mohiuddin, "Artificial neural networks: A tutorial", *IEEE Computer*, vol. 29, no. 3, pp. 31-44, 1996.

[47] M. H. Beale, M. T. Hagan, and H. B. Demuth, *Neural Network Toolbox: User's Guide*, MathWorks, 2017.

[48] A. E. Walsh and P. Gehringer, *Java 3D API Jump-Start*, Prentice Hall, 2002.